Synthesis and Crystal Structure of bis [2-(3-(2-((2-Hydroxybenzylidene) Amino)Ethyl)Oxazolidin-2-yl)Phenol]Cerium (IV) 1,4-Dioxane Monosolvate

G.Y.S.K. Swamy & P. Sivanarayanan

Taylor & Francis
Taylor & Francis Group

Synthesis and crystal structure of bis [2-(3-(2-((2-hydroxybenzylidene) amino)ethyl)oxazolidin-2-yl) phenol]cerium (iv) 1,4-dioxane monosolvate

G.Y.S.K. Swamy and P. Sivanarayanan

Center for X-ray Crystallography, CSIR-Indian Institute of Chemical Technology, Hyderabad, India

ABSTRACT

The metal complex, bis [2-(3-(2-((2-hydroxybenzylidene)amino)ethyl) oxazolidin-2-yl)phenol]cerium(IV) 1,4-dioxane monosolvate was synthesized and characterized by infrared, ^{1}H NMR, elemental analysis, single-crystal, and powder X-ray diffraction. The coordination polyhedra of cerium shows a distorted square-antiprismatic geometry. No classical hydrogen bonds were observed. The crystal packing was influenced by weak C-H···O (intermolecular) and van der Waals interactions.

1. Introduction

Tetravalent cerium compounds received much attention due to their high oxidation potential and multiple applications [1,2] in particular biological systems, where they show high reactivity [3]. Also, cerium (IV) is very interesting lanthanide that forms compounds in the tetravalent as well as the trivalent oxidation state. Its chemical behavior as a tetravalent metal is similar to those of Zr, Hf, Th, U, Np, and Pu. Further, complexes of Schiff base (salen-type) ligands with lanthanides were studied in the recent past [4–8]. In our previous papers, we investigated the coordination ability of the multidentate ligand (*N*-salicylidene-*N'*-(2-hydroxyethyl) ethylenediamine (*L*)) with copper (II), chromium (III), and indium (III) [9–11]. Since this ligand (*L*) has the strong coordination ability with various metals, we thought of trying with lanthanides and study their coordination environment. In that attempt, herein we report the synthesis and crystal structure of cerium(IV) coordination complex.

2. Experimental

2.1. *Materials and physical measurements*

All materials and reagents were obtained commercially and used without purification. The elemental analysis of C, H, and N were carried out using American PE2400 II CHNS/O

---

elemental analyzer. Infrared (IR) spectra were recorded on a Nicolet 5DXB Fourier transform-IR spectrophotometer in the region 4000–400 cm^{-1}, using KBr pellet. Electrospray ionization-mass spectra (ESI-MS, positive ion mode) were recorded with Exactive Orbitrap mass spectrometer (Thermo Scientific, Waltham, MA, USA). The samples were introduced into the source by flow injection using MeOH/H$_2$O (80:20) as the mobile phase at a flow rate of 600 µL/min. ^{1}H NMR spectra were measured with Bruker AVANCE-500 MHz spectrometer at ambient temperature in CD$_3$OD. Powder X-ray diffractograms were recorded on a Bruker-AXS D8-Advance, X-ray diffractometer with graphite-monochromated Cu-Kα radiation (λ = 1.5406Å) and 2θ ranging from 5° to 40° with step size 0.005° and step time 13.5 sec. The diffractometer is attached with high sensitive Lynx-Eye detector.

2.2. Preparation of bis [2-(3-(2-((2-Hydroxybenzylidene)Amino)Ethyl)Oxazolidin-2-Yl)Phenol] Cerium(Iv) 1,4-dioxane monosolvate complex (I)

The complex was prepared by dissolving equimolar (2 mmol) salicylaldehyde and N-(2-hydroxyethyl)ethylenediamine in methanol. After stirring for 10 min, a yellow color solution was obtained. To this solution was added Ce(NO$_3$)$_3$.6H$_2$O (2 mmol, in methanol) + 5 mL of 1,4-dioxane and the stirring continued for another 30 min. Upon slow evaporation, pale yellow color crystals were obtained at room temperature (Scheme 1)
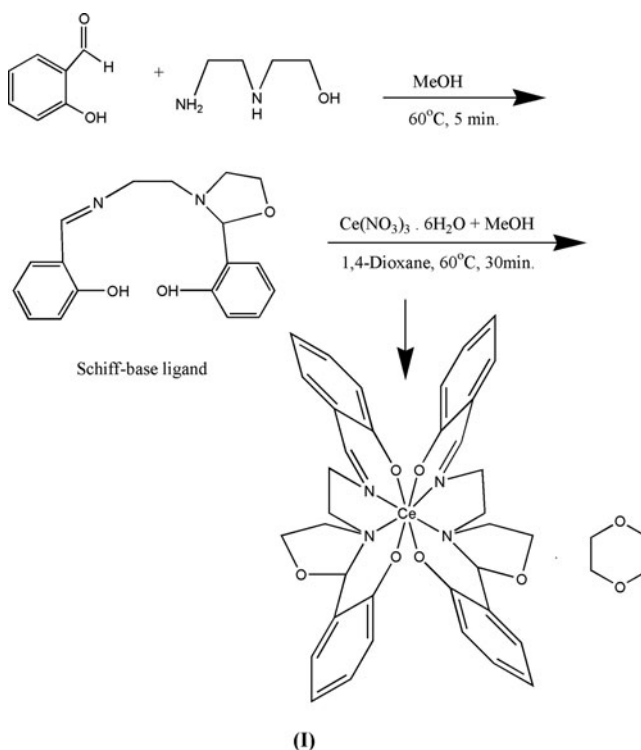
Scheme 1. Formation of Schiff base ligand and Ce(IV)-Schiff base complex.

Table 1. Crystallographic data and data collection parameters.

Empirical formula	$C_{40}H_{44}CeN_4O_8$
Formula weight	848.93
Crystal system	Orthorhombic
Space group	$P2_12_12_1$
Unit cell dimensions	$a = 10.8465(11)$ Å
	$b = 15.2253(15)$ Å
	$c = 23.2001(23)$ Å
V	3831.3(7) Å^3
Z	4
D_{cal}	1.4717 Mg/m^3
μ	1.245 mm^{-1}
Radiation (Mo $K\alpha$)	0.71073 Å
$F(000)$	1736
θ range for data collection	1.60–25.00°
Reflections collected	36,616
Independent reflections	6753
No. of reflections [$I > 2\sigma(I)$]	621
No. of parameters	478
Final R indices R/wR	0.0470/0.1030
Goodness of fit on F^2	1.134
Largest difference peak and hole (e Å^{-3})	1.186, −0.814

2.3. *Crystal structure determination and refinement*

X-ray single crystal data collected were performed at room temperature with a Bruker SMART Apex CCD area detector [12]. Preliminary lattice parameters and orientation matrices were obtained from three sets of frames. Intensity data were collected using graphite-monochromated Mo$K\alpha$ radiation ($\lambda = 0.71073$Å) with the ω-scan method.

Integration and scaling of intensity data were accomplished using SAINT [13] and absorption corrections were performed using SADABS [14]. The structures were solved by direct methods and refined by a full matrix least-squares procedure based on F^2 [15]. Nonhydrogen atoms were refined with anisotropic displacement parameters and hydrogen atoms were included in the models in their calculated positions in the riding model approximation. The details of the crystal data and refinement convergence are gathered in Table 1. The geometrical calculations and molecular graphics were computed using programs PARST [16], ORTEP-3 [17], and PLATON [18]. Additional information (CIF details) is available.

3. Results and discussion

3.1. *Spectroscopic properties*

For the title complex, the IR spectra of the ligand (Schiff base) and the metal-complex recorded separately (Figs. S1 and S2, supporting information). The characteristic phenolic γ(O-H) due to the presence of hydroxyl group in the ligand was observed in the region 3300–3500 cm^{-1}. The band appeared at 3419 cm^{-1} in the complex may be attributed to some moisture in the sample. The phenolic γ(C-O) stretching vibration appeared at 1278 cm^{-1} in the ligand was shifted to higher frequency, 1301 cm^{-1} after complexation. This shift confirms the participation of phenolic oxygen in C-O-M bond formation [19]. The characteristic band of the Schiff base appeared at 1662 cm^{-1} (γC = N stretching) underwent a bathochromic shift to lower frequency 1595 cm^{-1} in the complex. This redshift indicates that the imino nitrogens of the ligand are coordinated to metal atom [20]. In the low frequency region of the complex spectrum, the presence of sharp intensity bands in the region 600–450 cm^{-1}, which

Table 2. Elemental analysis of $C_{40}H_{44}CeN_4O_8$.

Element	Experimental(%)	Calculated(%)
Carbon	56.38	56.60
Nitrogen	6.51	6.60
Hydrogen	5.22	5.19

can be attributed to metal-nitrogen (γM-N) and metal-oxygen (γM-O) stretching vibrations, respectively [21].

3.2. *Elemental analysis*

In order to confirm the chemical composition of the synthesized compound, carbon, hydrogen, and nitrogen (C, H, and N) analysis was carried out. The experimental and calculated values of C, H, and N are given in Table 2. The difference between experimental and calculated values of C, H, and N were very close to each other and within the experimental errors. This confirms the formation of the product in the stoichiometric ratio.

3.3. *ESI-mass spectra*

The positive ion ESI mass spectrum (Fig. S3) of the prepared Ce(IV)-complex showed the protonated molecule, $[M+H]^+$ at m/z 761. This species corresponds to the $[Ce+2L+H]^+$ ion (without 1,4-dioxane solvent). The isotopic distribution of the ion m/z 761 matching well with the simulated spectrum obtained for $[C_{36}H_{36}N_4O_6Ce]^+$. The spectrum clearly confirms the formation of the complex as observed by X-ray diffraction.

3.4. *^{1}H NMR spectral analysis*

The ^{1}H NMR spectrum of the crystal structure was shown in Fig. S4. The spectrum showed two sharp singlets at $\delta =$ 8.34 and 5.67 ppm due to two protons (s:1H and 1H) attached to atoms C7 and C12 of the Ce(IV) complex, respectively. The signals for aromatic region appeared between $\delta =$ 5.9–7.45 ppm in the form of a doublet at $\delta =$ 5.88 ppm (d, $J =$ 8.1 Hz, 1 H); two triplets at $\delta =$ 6.95 (t, $J =$ 7.7 Hz, 1 H), 6.49 ppm (t, $J =$ 7.4 Hz, 1 H), and three multiplets in the regions, $\delta =$ 6.63–6.70 (m, 2H), 7.25–7.28 (m, 2H), and 7.36–7.40 ppm (m, 1H). The signals correspond to the ethylenediamine in the complex molecule yielded three multiplets in the regions $\delta =$ 3.95–4.0 (m, 2H), 4.05–4.12 (m, 2H), and 4.35–4.42 ppm (m, 2H) and one doublet of doublet at $\delta =$ 4.23 ppm (dd, $J =$ 7.5, 15.7 Hz, 2 H). The protons resonated as a multiplet in the region $\delta =$ 5.12–5.19 ppm (m, 4H) correspond to the uncoordinated 1,4-dioxane solvent molecule. The total number of protons (22) matches well with the X-ray structural data (one half of the symmetry related molecule).

3.5. *Description of the crystal structure*

Figure 1 shows an ORTEP drawing of (I) with atomic numbering scheme which was drawn at 30% probability level using PLATON. Selected bond distances and angles are given in Table 3. The structure consists of the neutral asymmetric unit that comprises a cerium(IV) complex
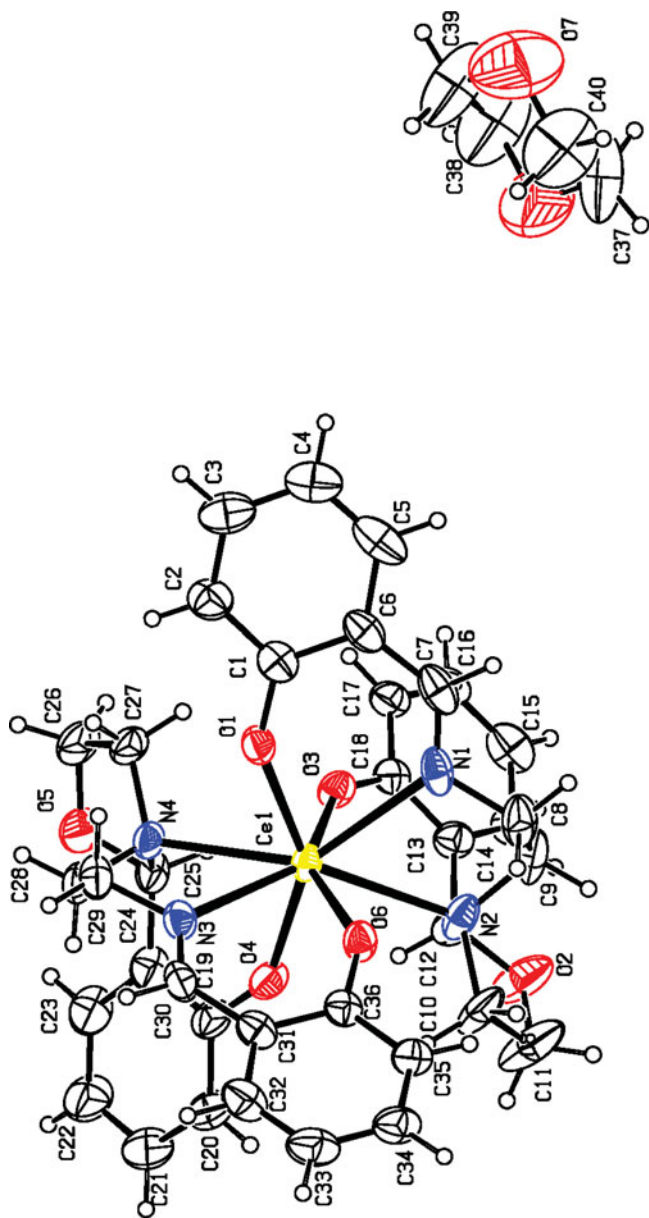
Figure 1. Structural representation and atom-numbering scheme of (I). Displacement ellipsoids are drawn at 30% probability level.

Table 3. Selected geometric parameters [Å, °].

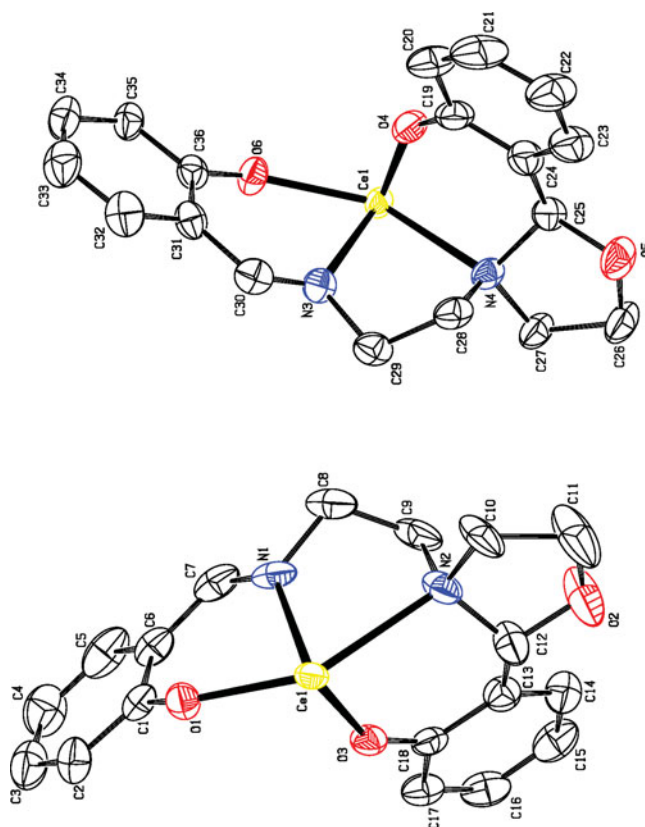|			
Ce1-N1	2.561 (6)	Ce1-O3	2.194 (4)
Ce1-N2	2.683 (5)	Ce1-O4	2.204 (5)
Ce1-N3	2.573 (5)	Ce1-O6	2.181 (4)
Ce1-N4	2.662 (5)	C7-N1	1.290 (10)
Ce1-O1	2.216 (4)	C30-N3	1.271 (8)
N1-Ce1-N2	66.71 (2)	N2-Ce1-N3	139.74 (15)
N2-Ce1-N4	132.66 (15)	N3-Ce1-N4	66.43 (16)
N3-Ce1-O3	143.48 (15)	N4-Ce1-O1	78.03 (15)
O1-Ce1-O3	93.20 (15)	O3-Ce1-O4	91.90 (16)
O4-Ce1-O6	92.37 (16)	O1-Ce1-O4	145.42 (16)

Figure 2. ORTEP drawings (30% probability) of the two halves of the Ce(IV)-complex molecule, which are almost identical. H atoms have been omitted for clarity and atoms of the 1, 4-dioxane molecule were not included.

and a solvent 1,4-dioxane molecule of crystallization in a 1:1 ratio. Figure 2 shows individual halves of the complex (without solvent molecule, 1,4-dioxane), which are near identical. The Ce atom has an eight-coordinate geometry involving two tetradentate [2-(3-(2-((2-hydroxybenzylidene)amino)ethyl)oxazolidin-2-yl)phenol] ligands with an average Ce-N distance of 2.620(5) SÅ and Ce-O distance of 2.199(4) Å. The geometrical parameters data are comparable with the related structures [22–25].

Using the "shape measure" concept [26–29], we have measured the shape of the polyhedron in terms of a parameter "S" (the minimal variance of the dihedral angles along all the edges of a polyhedron) (Supplementary Tables S1 and S2). This can be defined as: $S(\delta, \theta) = min[((1/m) \sum (\delta_i - \theta_i)^2)^{1/2}]$ where m, δ_i, and θ_i are the number of possible edges (18 in the present study), the observed dihedral angle between planes of the ith edge of the experimental polyhedron (δ) and the corresponding ideal structure (θ). The values found for the shape measures are $S(D_{2d})$ (corresponds to trigonal dodecahedron (TDH) geometry) = 11.82° and $S(D_{4d})$ (corresponds to square antiprism (SAP) geometry) = 7.75°. These values of S show that the coordination geometry around the Ce(IV) ion deviates significantly from an ideal polyhedron. The lower shape measure for the D_{4d} comparison suggests that the coordination polyhedron is closest to an idealized SAP geometry. We have compared the coordination environment of Ce(IV) (present one) with some Ce(III)/Ce(IV) [28,30–33] complexes (eight coordination) in the literature. We noticed that the distortion from the idealized polyhedron

Table 4. Hydrogen bonding geometry [Å,°].

D-H···A	D-H	H···A	D···A	D-H···A
C3-H3···O6[i]	0.93	2.72	3.625	164.9 (6)
C5-H5···O6[ii]	0.93	2.71	3.261	119.0 (5)
C35-H35···O5[iii]	0.93	2.68	3.58	161.3 (4)

Note: Symmetry code: (i) $x-\frac{1}{2}$, $-y+\frac{1}{2}+1$, $-z$; (ii) $-x+2$, $y-\frac{1}{2}$, $-z+\frac{1}{2}$; and (iii) $x+1$, y, z.

depends on mainly two factors. One is, the coordination environment and the other, hydrogen bonding (packing of the molecule). It hardly depends on the type of metal or its ionic nature. For example, Xu et al. [28] observed that the solvent hydrogen bonding and molecular packing make a considerable impact on the distortion of metal coordination environment. The same has been observed in another two Ce(III) complexes, $[Ce(DMSO)_8](BPh_4)_3$ [30] and $[Ce(C_2H_6OS)_8]_2[MoO_{19}]_3.4C_2H_6OS$ [31], where the Ce-O distances (average) are 2.472 (in the previous one) and 2.471 $S\text{Å}$ (later one), which are very close to the ideal value (sum of the covalent radii, Ce-O, 2.490 Å). While the geometry of the coordination polyhedron of Ce(III) in $[Ce(DMSO)_8](BPh_4)_3]$ is tetragonal antiprism, the other one has a distorted square antiprism. The geometrical distortion in the later might be due to the hydrogen bonding and the crystal packing, as mentioned above.

The bonds Ce1-N2 and Ce1-N4 are longer than the corresponding Ce1-N1 and Ce1-N3 by nearly 0.1 Å (Table 3). This stretching may be attributed to the ring puckering of the respective oxazolidine ring. The least-squares planes (C1-C18, O1, O2, O3, N1, and N2; C19-C36, O4, O5, O6, N3, and N4) containing the ligands are oriented at an angle 31.2(1)° to each other. The intramolecular dihedral angles between the aromatic rings (C1-C6 & C13-C18;
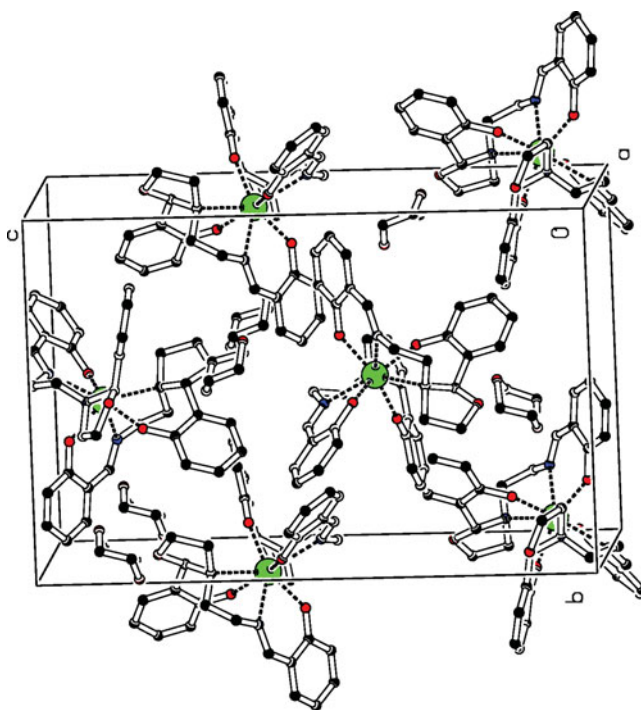

Figure 3. A portion of the crystal structure of (I), projected along the *c*-axis. H atoms have been omitted for clarity.
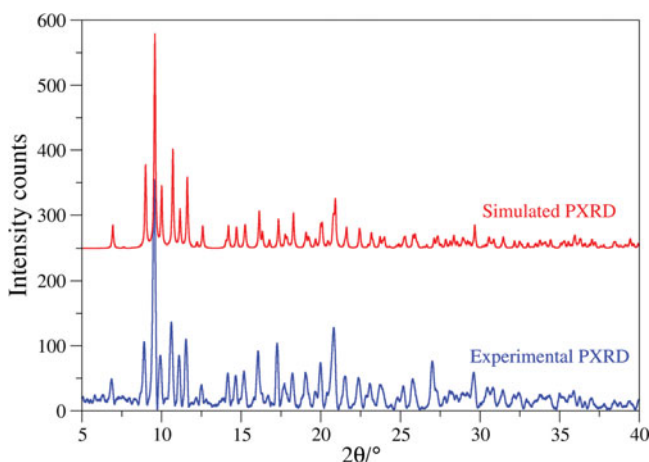
Figure 4. Simulated and experimental PXRDs of Ce(IV)-Schiff base complex.

C19-C24 & C31-C36) are 59.4(3)° and 52.2(2)°, respectively. The five-membered oxazolidine rings (N2, O2, C10-C12 and N4, N5, C25-C27) in both the ligands, puckered with envelope conformation (ΔC_S (C12) = 11.31 and ΔC_S (C25) = 6.07, respectively).

The structure contains a number of intermolecular C-H···X contacts with H···X being well within the van der Waals radii (those with C-H···X angle above 100° are listed in Table 4). No classical hydrogen bonds were found in the structure (Fig. 3). The intermolecular contacts may be regarded as weak nonclassical C-H···O hydrogen bonds, but their contribution to the overall lattice energy must be very small. The structure was stabilized by C-H···O and van der Waals interactions.

3.6. *PXRD measurement*

The results of the simulated and experimental powder X-ray diffractogram (PXRD) patterns of Ce(IV)-complex (I) are in good agreement with each other (Fig. 4), thus indicating that the single crystals of (I) studied represent the respective bulk material. Also found a few additional peaks and some differences in the intensities between the peaks of the patterns (experimental and simulated). This may be attributed to a very minor quantity of an impurity phase and the effect of preferred orientation of the powder sample.

Acknowledgments

References

[1] Binnemans, K. (2006). In *Handbook on Physics and Chemistry of Rare Earths*, Chapter 229. Gschneidner, K. Jr., Bunzli, J.-C. & Pecharsky, V. (Eds.), Elsevier: North Holland, 36.
[2] Nair, V., Balagopal, L., Rajan, R., & Mathew, J. (2004). *Acc. Chem. Res.*, 37, 21.

[3] Sigel, A., & Sigel, H. (Eds). (2003). *Metal Ions in Biological Systems*, Marcel Dekker, Inc.: New York, Basel, 40.

[4] Evans, W. J., Fujimoto, C. H., & Ziller, J. W. (1999). *Chem. Commun.*, 1999, 311.

[5] Evans, W. J., Fujimoto, C. H., & Ziller, J. W. (2002). *Polyhedron*, 21, 1683.

[6] Baleizao, C., & Garcia, H (2006). *Chem. Rev.*, 106, 3987.

[7] You, Z. -L., Shi, D. -H., Xu, C., Zhang, Q., & Zhu, H. -L. (2008). *Eur. J. Med. Chem.*, 43, 862.

[8] Meermann, C., Sirsch, P., Tornroos, K. W., & Anwander, R. (2006). *Dalton Trans.*, 8, 1041.

[9] Swamy, G. Y. S. K., Ravikumar, K., Chandramohan, K., & Lakshmi, N. V. (2001). *Cryst. Res. Technol.*, 36(11), 1273.

[10] Swamy, G. Y. S. K., & Ravikumar, K. (2008). *Anal. Sci.*, 24, x161.

[11] Swamy, G. Y. S. K., & Ravikumar, K. (2011). *J. Struct. Chem.* 52, 208.

[12] Bruker *SMART (Version 5.625)*. (2001). Bruker AXS Inc.: Madison, Wisconsin, U.S.A.

[13] Bruker *SAINT (Version 6.28a)*. (2001). Bruker AXS Inc.: Madison, Wisconsin, U.S.A.

[14] Sheldrick, G. M. (1996). *SADABS. Program for Empirical Absorption Correction of Area Detector Data*, Univ. of Gottingen: Germany.

[15] Sheldrick, G. M. (1997). *SHELXS97* and *SHELXL97*, *Programs for Crystal Structure Solution and Refinement*, University of Gottingen: Germany.

[16] Nardelli, M. J. (1995). *J. Appl. Cryst.*, 28, 659.

[17] Farrugia, L. J. (1997). *J. Appl. Cryst.*, 30, 565.

[18] Spek, A. L. (2003). *J. Appl. Cryst.*, 36, 7.

[19] Satyaraj, S., Butcher, R. J., & Jayabalakrishnan, C. (2013). *J. Coord. Chem.*, 66, 580.

[20] Ajibade, P. A., Kolawole, G. A., O'Brien, P., Helliwell, M., & Raftery, J. (2006). *Inorg. Chim. Acta.*, 359, 3111.

[21] Nakamoto, K. (1997). *Infrared and Raman Spectra of Inorganic and Coordination Compounds*, 5th ed., Wiley: New York.

[22] Drose, P. et al. (2011). *Z. Anorg. Allg. Chem.*, 637, 369.

[23] Liu, Y.-F., Xia, H.-T., Wang, D.-Q., & Yang, S.-P. (2007). *Acta Cryst.*, E63, m484.

[24] Yang, S.-P., Han, L.-J., Wang, D.-Q., & Wang, B. (2007). *Acta Cryst.*, E63, m2777.

[25] Timmons, J. H. et al. (1980). *Inorg. Chem.*, 19, 3553.

[26] Porai-Koshits, M. A., & Aslanov, L. A. (1974). *Russ. J. Struct. Chem.*, 13, 244.

[27] Kepert, D. L. (1978). *Prog. Inorg. Chem.*, 24, 179.

[28] Xu, J., Radkov, E., Ziegler, M., & Raymond, K. N. (2000). *Inorg. Chem.*, 39, 4156.

[29] Miyata, K. et al. (2011). *Chem. Eur. J.*, 17, 521.

[30] Sakiyama, H., Yuzawa, H., Yoshioka, D., & Mikuria, M. (2014). *X-ray Structure Analysis Online*, 30, 19.

[31] Khelifa, A. B., Giorgi, M., & Belkhiria, M. S. (2012). *Acta Cryst.*, E68, m938.

[32] Abbasi, A. et al. (2007). *Inor. Chem.*, 46, 7731.

[33] Wang, X. et al. (2003). *Inorg. Chem.*, 42, 4135.